

RESEARCH

Open Access



Resilience and systems- A traffic flow case example

Khalilullah Mayar^{1*}, David G. Carmichael¹ and Xuesong Shen¹

Abstract

Resilience has increasingly become a crucial topic to the function of various real-world systems as our planet undergoes a rising trend of uncertainty and change due to natural, human and technological causes. Despite its ubiquitous use, the term resilience is poorly and often inconsistently used in various disciplines, hindering its universal understanding and application. This study applies the resilience system interpretation framework, which defines resilience irrespective of its disciplinary association, in the form of adaptation and adaptive systems, to two traffic flow systems. The system framework defines resilience as the ability of the system state and form to return to their initial or other suitable state or form through passive and active feedback structures. Both components of the system framework are demonstrated through practical simulation scenarios on the modified viscous Burgers' equation and the LWR-Greenshields model equipped with an adaptive Extremum seeking control, respectively. This novel and systematic understanding of resilience will advance resilience analysis, design, and measurement processes in various real-world systems in a unified fashion and subsequently pave the way for resilience operationalization and its integration into industry standards.

Highlights

- A novel system definition for resilience and its constituent elements in the form of adaption is presented.
- The system framework is subsequently applied to two simple traffic flow systems.
- Modified viscous Burgers' equation and LWR-Greenshields model equipped with an adaptive Extremum seeking control demonstrate the passive and active feedback structures as the two tools for obtaining system resilience.
- This cross-disciplinary system framework offers the potential for a greater understanding of resilience, eliminates overlap, and paves the way toward resilience operationalization.

Keywords Traffic flow, Extremum seeking control, Dynamic stability, Passive control, Active control, Resilience, System thinking, Modern control systems theory

*Correspondence:

Khalilullah Mayar
k.mayar@unsw.edu.au

¹School of Civil and Environmental Engineering, The University of New South Wales, 2052 Sydney, NSW, Australia



© The Author(s) 2024. **Open Access** This article is licensed under a Creative Commons Attribution 4.0 International License, which permits use, sharing, adaptation, distribution and reproduction in any medium or format, as long as you give appropriate credit to the original author(s) and the source, provide a link to the Creative Commons licence, and indicate if changes were made. The images or other third party material in this article are included in the article's Creative Commons licence, unless indicated otherwise in a credit line to the material. If material is not included in the article's Creative Commons licence and your intended use is not permitted by statutory regulation or exceeds the permitted use, you will need to obtain permission directly from the copyright holder. To view a copy of this licence, visit <http://creativecommons.org/licenses/by/4.0/>.

Introduction and background

This paper applies the resilience system interpretation framework to a traffic flow system that is subjected to perturbations and change. The system framework employed defines resilience in the form of adaptation and adaptive systems, where the system has the ability to respond to perturbations and change through passive and active feedback structures [1]. The modified viscous Burgers' equation and the Lighthill-Whitham-Richards (LWR)- Greenshields model, coupled with an adaptive Extremum seeking control (ESC), for two macroscopic traffic-flow systems are used in a state-space representation; the system response to perturbation and change is first simulated, and then its resilience characteristics are analyzed.

Over the years, numerous studies have been conducted with a focus on traffic flow systems management and their response to disruptive events and congestions using systems and modern control systems approaches. Some of those system approaches use the transportation system's physical features [2, 3] while others use the system's traffic flow characteristics [4–6] in defining their systems' resilience frameworks. Among those, adaptive control mechanisms, such as machine learning in traffic signals control at ramps and intersections [7–11], model reference adaptive control in car following [12] and real-time traffic management [13], model predictive control in urban traffic management [14–18], extremum seeking control in traffic congestion and lane-changing management [19, 20], adaptive fuzzy control in traffic flow ramp metering and signal optimization [21–24], as well as other fixed control schemes such as optimal control [20, 21] and linear quadratic control [22, 23], have been widely applied. However, the majority of the literature fails to establish systematic linkages among the passive and active feedback structures utilized by the system to obtain resilience - described in terms of adaptability with system state and form return abilities. The resilience system interpretation framework introduced by Mayar et al. [1] defines resilience as adaptability and adaptive systems where the system under perturbations and change has the ability to return to a starting or other suitable state or form through the system passive and active feedback mechanisms respectively. The framework was first

applied to two simple linear and nonlinear dynamic systems [25] and a building structure system [26] and this study extends the resilience system interpretation framework application to a traffic flow system - proving the framework universal application to various engineering disciplines and therefore making an original contribution to the field.

The study is structured as follows: section “[Methodology and analysis tools](#)” provides an introduction to the methodological framework for the two macroscopic traffic flow systems and their constituent elements including perturbations and change. Section “[Resilience as system interpretation](#)” analyzes the resilience system interpretation under the two broad categories; system state and form and their abilities to return to their initial or other suitable states and forms. Lastly, section “[Discussion and conclusions](#)” presents a summary and discussion.

Methodology and analysis tools

The methodological framework utilized in the study is a state-space approach from modern control systems theory where the system's fundamental variables are the system input (control and disturbance), state (system internal behavior), and output (system external performance or response) (Fig. 1), which accommodates both the system's passive and active feedback features.

The term system here is defined as a set of interacting or interrelated components (or subsystems) isolated from the external environment by its boundary, which is freely chosen by the observer to better serve the purpose of the target study [27]. A transportation system model is generally comprised of three main components: (1) travel demand and user behavior (demand models), (2) transportation services and their functioning (supply or performance models), and (3) the interaction of the two (assignment models) [28]. In this study, the selected transportation models are limited to the traffic flow models that fall under the supply or performance component. Several constraints have been imposed for the sake of simplicity such as a single section or link of a road instead of a road network, as well as an initial fixed amount of demand flow and a pre-trip path choice.

In a system methodology, particularly a state-space approach, the first crucial step is to define the system,

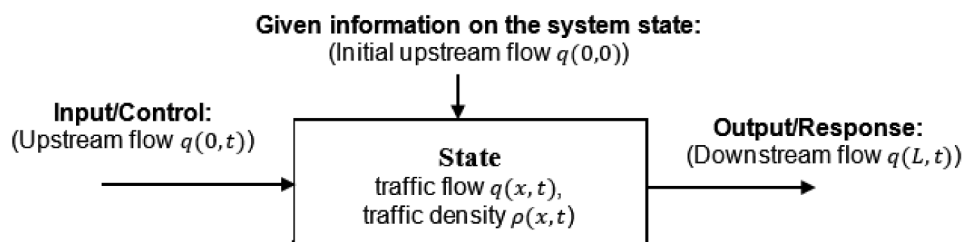


Fig. 1 Traffic flow system single-level system representation

which entails determining the system boundary, its fundamental variables, and the relevant constituting subsystems. A system can be described both in a single-level (Fig. 1) or a multi-level (subsystem) of details (Fig. 2). The subsystems for a traffic flow system can be arranged in the form of four hierarchical interacting layers of structure, member, element, and material, as introduced by Carmichael [29] in the context of structural analysis (system multi-level representation). The behavior of each subsystem is defined in terms of a constituent relationship (similar to a stress-strain equation), while their interaction is defined by equilibrium (similar to a force-stress equation) and compatibility relationships (similar to a strain-displacement equation) [29, 30]. The traffic flow system's constituent layers consist of single-vehicle movement, microscopic traffic flow, mesoscopic traffic flow, and macroscopic traffic flow layers (Fig. 2). The fundamental variables of each subsystem are functions of time and space (both independent variables). For the single vehicle movement or material layer, the system model is described by the kinematic equations of the motion, which can be rewritten in the form of ordinary differential equations. The system state is subsequently defined by a dual-tuple of $(v(t) - \text{velocity and } a(t) - \text{acceleration})$, output $(v(t))$ and the control variable as the vehicle jerk (j) and/or the force (F) exerted on the gas pedal. The microscopic traffic flow or element layer describes the interaction of adjacent vehicles in a traffic stream with

each other and with the road infrastructure [31, 32]. The subsystem models are defined by the ordinary differential equations and the system state is determined by a dual-tuple of $(\Delta x(t), \text{ the following vehicle's relative position and } \Delta v(t), \text{ the following vehicle's relative velocity with regard to the leading vehicle})$, output $(\Delta x(t))$ and the following vehicle's acceleration as the control variable $(a(t))$. The mesoscopic traffic flow or member layer, acts as a middle ground and connection between the microscopic and macroscopic models by combining the individual vehicles' velocities through probability distribution functions on a microscopic level with flow and density from a macroscopic level [32–34]. The macroscopic traffic flow or structure level considers traffic as a continuum of fluid flow, assuming the law of conservation of flow, which means that no vehicle can (dis)appear within a certain stretch of road. The analogy between traffic flow and fluid flow is based on the fair resemblance of heavy traffic flow to a fluid stream— considering a macroscopic traffic flow as a one-dimensional compressible fluid [35]. The subsystem models for a macroscopic traffic flow are defined by partial differential equations and the system is determined by a dual-tuple of the $(q(x, t) - \text{flow and } \rho(x, t) - \text{density})$, output (downstream flow), and the control variable as the upstream flow and/or free flow velocity (v_f) (Fig. 2). In this study, the traffic flow system behavior is investigated on the aggregate and structure level, and a single-level system representation is adopted

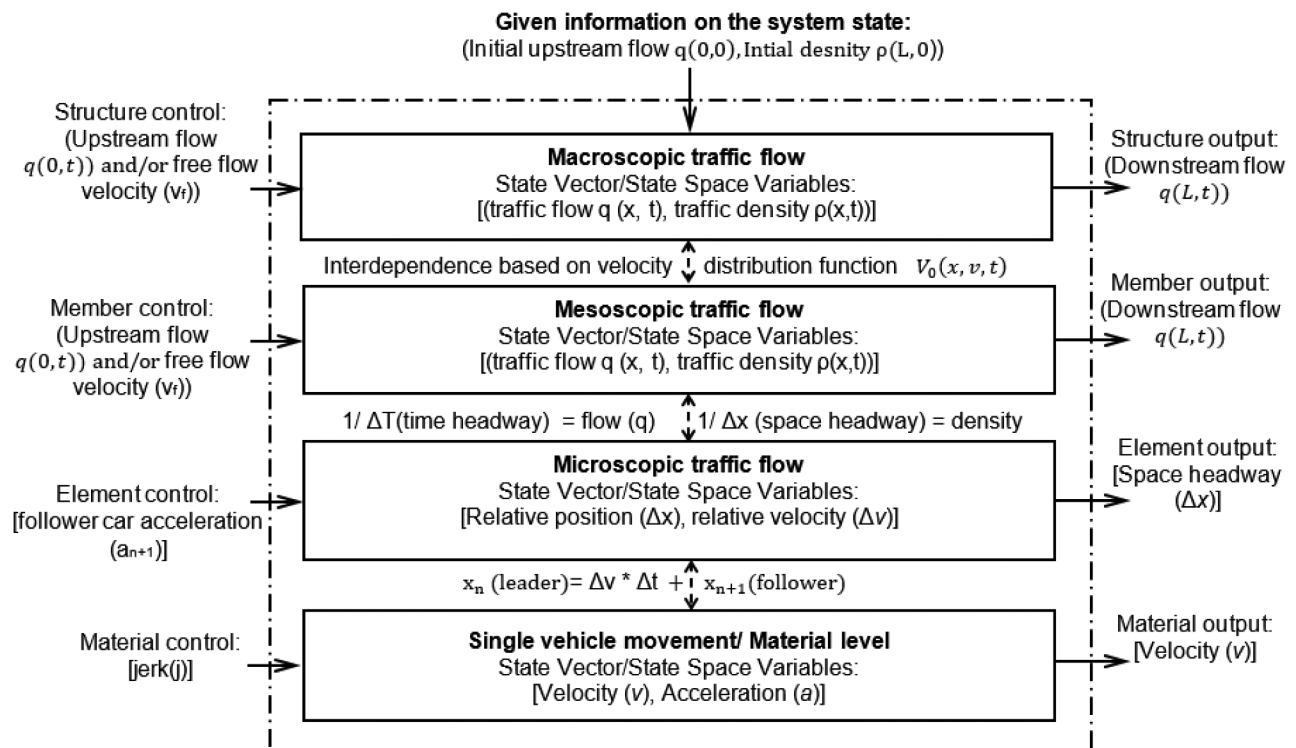


Fig. 2 Traffic flow system boundary and hierarchical multi-level representation in a control system theory– state space approach setting

accordingly (Fig. 1). The control systems theory in general and the state-space approach in particular adopted here, possesses both the conceptual and practical power to accommodate various system level representations as well as the interactions across its various layers. The critical challenge of the task is defining the system and its relevant constituent elements in terms of input, state and output as per the study objectives.

The analysis examples selected for this study consist of the modified viscous Burgers' Equation, which is a non-equilibrium macroscopic flow model that has the inherent ability to handle perturbations within the flow, and the Lighthill-Whitham-Richards (LWR)-Greenshields model, an equilibrium model with no inherent ability to handle perturbations and change unless an active feedback structure is incorporated within the system. The perturbation event for the modified viscous Burgers' equation is introduced in the form of a modified unit pulse function that indicates an abrupt temporary drop in the traffic flow or, alternatively, an abrupt temporary increase in the traffic density, which is a common indication of disruptions such as bottlenecks, traffic accidents and stoplights (Fig. 3). The analysis tools utilized in these studies are theoretical numerical simulations carried out on perturbation events data generated by their respective functions demonstrating real-life traffic scenarios such as bottlenecks and traffic accident sites.

Modified viscous burgers' equation

Contrary to the equilibrium models (LWR model in section "Lighthill-Whitham-Richards (LWR) Model and Extremum Seeking Control"), non-equilibrium macroscopic traffic flow models, also known as higher-order relations can better describe real-world traffic scenarios by accommodating perturbed traffic flows. One of the well-known non-equilibrium models is the general viscous Burgers' Equation from fluid mechanics, which is the result of adding a smooth dispersion term ($D\partial_x^2\rho$) to the conservation equation (LWR model) (Eq. 1). If the characteristic slope $q'(\rho)$ is replaced with an equivalent density term (ρ) the resulting equation is called the general viscous Burgers' Equation (Eq. 2).

$$\partial_t\rho + q'(\rho)\partial_x\rho = D\partial_x^2\rho \tag{1}$$

$$\partial_t\rho + \rho\partial_x\rho = D\partial_x^2\rho \tag{2}$$

In order to make the general viscous Burgers' equation model precisely suited to describe a real-world traffic flow phenomenon, the $q'(\rho)$ term is replaced by the traffic Greenshields constituent equation (Eq. 3) and, as a result, a modified viscous Burgers' equation emerges (Eq. 4).

$$\partial_t\rho + \left[v_f \left(1 - \frac{2\rho}{\rho_{jam}} \right) \right] \partial_x\rho = D\partial_x^2\rho \tag{3}$$

$$\partial_t\rho + v_f\partial_x\rho - 2v_f\frac{\rho}{\rho_{jam}}\partial_x\rho = D\partial_x^2\rho \tag{4}$$

In Eqs. (1–4); ρ and q are the distributed traffic flow parameters of density and flow, v_f is the free flow velocity, ρ_{jam} is the jam density, $D = \frac{\mu}{\rho}$ is the kinematic viscosity and μ is the viscosity of the fluid.

Lighthill-Whitham-Richards (LWR) model and extremum seeking control

Equilibrium models, also known as first-order relations, can only describe unperturbed traffic flow and are based on the law of conservation of flow from fluid dynamics [36]. A famous example of this category is the Lighthill-Whitham-Richards (LWR) model that connects the distributed traffic flow parameters of flow $q(x, t)$, density $\rho(x, t)$ and speed $v(x, t)$ using a Partial Differential Equation (PDE) (Eq. 5) coupled with a fundamental equation (Eq. 6). The traffic dynamics are restricted to an equilibrium state curve, also known as a constituent equation (speed-density relation), which has a linear form in the case of the Greenshields model (Eq. 7) with a parabolic phase space for the two-state variables of flow and density (Fig. 4).

$$\frac{\partial\rho}{\partial t} + \frac{\partial q}{\partial x} = 0 \tag{5}$$

$$q = \rho v \tag{6}$$

$$v = v_f \left(1 - \frac{\rho}{\rho_{jam}} \right) \tag{7}$$

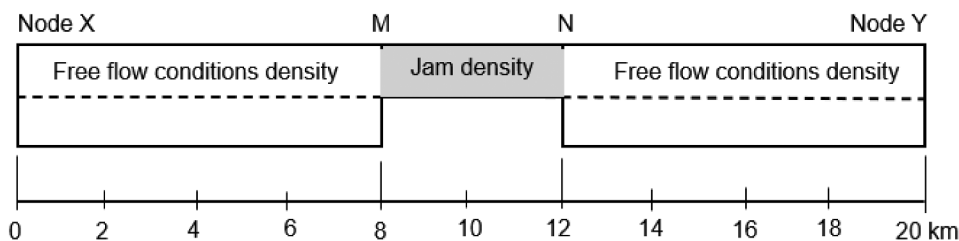


Fig. 3 Schematic illustration of a two-lane highway link traffic density with a bottleneck in the middle of the link

In Eqs. (6, 77), v is the space speed, which indicates the slope of the flow-density curve (Fig. 4) at each point of the curve ($v=\Delta q/\Delta\rho$). The scalar conservation law (Eq. 5) in its alternative form (Eq. 8), after plugging in the constituent (Eq. 7), takes on a quasilinear hyperbolic form (Eq. 9).

$$\rho_t + [q(\rho)]_x = 0 \quad \text{or alternatively} \quad \rho_t + q'(\rho) \rho_x = 0 \quad (8)$$

$$\rho_t + v_f \left(1 - \frac{2\rho}{\rho_{jam}} \right) \rho_x = 0 \quad (9)$$

Provided that the density (ρ) is one of the overall two state variables. The LWR model given by (Eq. 8) represents a state space equation where $q'(\rho)$ is, in fact, the system state matrix A (Eq. 10) of the system state-space with only one element and therefore it has one eigenvalue equal to the element itself (Eq. 11). $q'(\rho)$ is also called the characteristic slope. A characteristic is a straight line intersecting the x-axis at a point equal to the initial value of the density and the density along the characteristic line stays constant and equal to its initial value.

$$A = q'(\rho) = v_f \left(1 - \frac{2\rho}{\rho_{jam}} \right) \quad (10)$$

$$\lambda = q'(\rho) = v_f \left(1 - \frac{2\rho}{\rho_{jam}} \right) \quad (11)$$

The stability condition for an equilibrium state in the sense of asymptotic stability: the real part of the eigenvalue should be negative or zero [in a general Lyapunov stability sense] is given by (Eq. 12). The stability condition in (Eq. 12) reveals that for the traffic density to be stable and return to its usual state (state A– located anywhere between D and C in Fig. 4), it should be bounded to the ($\frac{\rho_{jam}}{2}$) upper limit (Point C). Any values for density (state variable) in the congestion (C-B) region is not recoverable from disruption unless an external intervention (active feedback) is implemented.

$$\lambda = v_f \left(1 - \frac{2\rho}{\rho_{jam}} \right) \leq 0 \quad \text{or} \quad \rho \leq \frac{\rho_{jam}}{2} \quad (12)$$

Figure 4 describes the changes to traffic flow in the LWR and Greenshields equilibrium model; portions of the plot shown with a black solid line indicate free flow/non-congested flow /stable flow conditions ($\lambda \leq 0$) while the portions shown with a black dotted line indicate congested flow/forced flow conditions. The point where free-flow conditions transition to congested flow conditions is the maximum point of the flow-density curve (condition C). At point C, the values of flow, density, and speed variables are critical ($q_{cr}, \rho_{cr}, v_{cr}$) and are considered to be the optimum values for traffic flow, indicating a saturated traffic flow state, after which the system state enters the congested traffic flow zone (curve portion shown with a black dotted line). ρ_{cr} is also called the maximum density

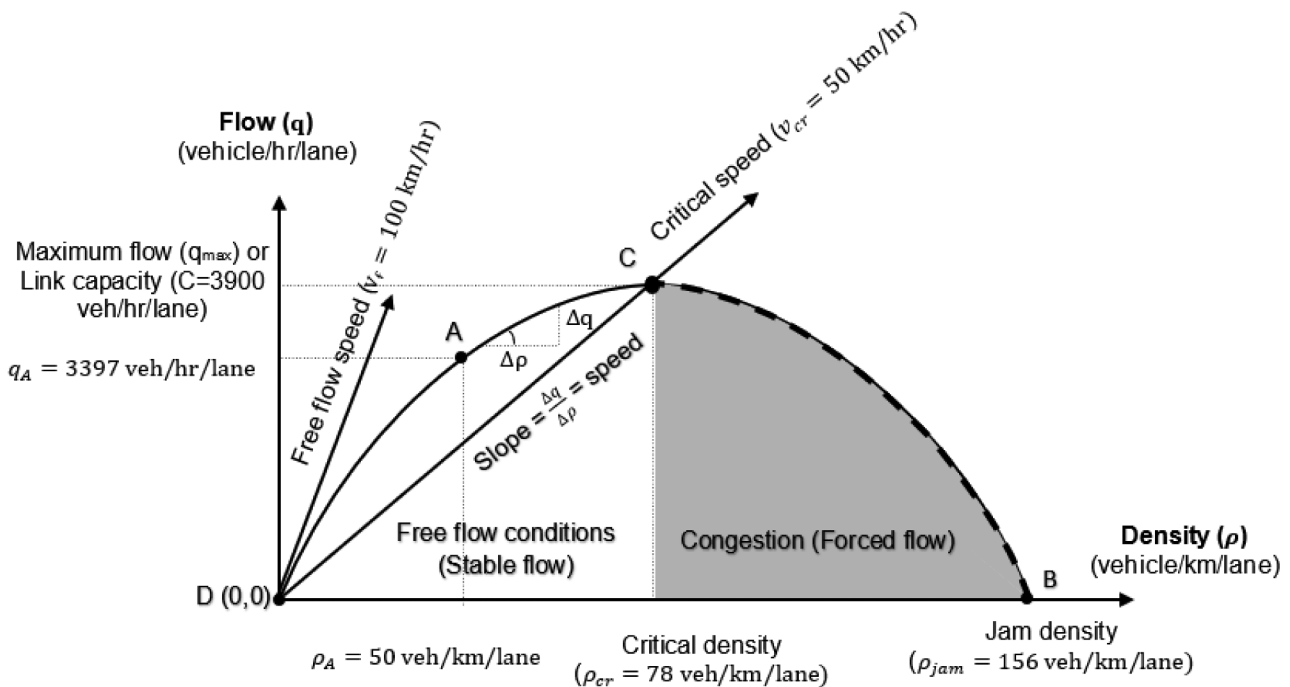


Fig. 4 Flow-density curve (phase space) for the Greenshields model: $q = 100\rho - \frac{100}{156}\rho^2$

under the free flow zone (curve portion shown as a solid black line) and is the limit for unforced recovery.

There are three major distinctive conditions/points (A, C, and D) on the flow-density curve and its associated density-speed, and speed flow diagrams. Point D is where both the traffic flow and density are very low (close to zero) and therefore vehicles travel at the highest speed limit, referred to as the free flow speed (v_f) without any interaction between two adjacent vehicles. Moving up toward point C the flow and density increase and the speed gradually decreases until point C is reached, which is the transition point between free flow and congested flow conditions. Moving down from point C toward point B results in a gradual decrease in both flow and speed values as the system state enters a congested flow region (adjacent leader and follower vehicles interact with each other). This decrease in flow and speed in turn results in a gradual increase in density until point B is reached, where both the flow and speed values become very low (zero) and result in the maximum density in a congested region (jam density). Any sudden increase in traffic density forces the system into the congested area (Points C to B) and creates shock waves (perturbation) that are mathematically represented by the model characteristic slope (Eq. 11).

Adaptive extremum seeking control (ESC), also known as an advance form of perturb and observe control, is an adaptive model-free active control structure that responds to changes in the system (underlying unknown dynamics) through input regulations for maximizing an objective function (a suitable form) [37]. ESC with a static objective function based on the Greenshields constituent equation is applied here to regulate the perturbed traffic flow system by adjusting the system's unknown dynamics (assumed to be following the LWR-Greenshields model) to conform to the perturbed state of the system in the bottleneck (Fig. 5).

Resilience as system interpretation

This Section numerically demonstrates the application of the resilience system interpretation framework to the two simple traffic flow systems. First, under perturbation, the ability of the system state to return to its initial or other suitable state through its passive feedback mechanism is simulated on a modified viscous Burgers' equation, subsequently, under change, the ability of the system form to return to its initial or other suitable form through its active feedback structure is simulated on the assumed LWR-Greenshields-based data coupled with an adaptive extremum seeking control.

Resilience as system state return ability

In order to envisage the system state's ability to return to its initial state or other suitable state, a simulation scenario is explored that entails normal vehicular traffic flow moving from node X toward node Y along a two-lane, one-way road section (Link XY of length $L=20$ km) (Fig. 3). Link XY has a maximum capacity (critical or optimum flow) of $q_{max} = 3900\text{veh/hr/lane}$, jam density of $\rho_{jam} = 156\text{veh/km/lane}$, critical or optimum density of $\rho_{cr} = 78\text{veh/km/lane}$, a free flow speed of $v_f = 100\text{km/hour}$. The traffic moves in a normal free flow condition at position A located on the left hand side of the Greenshields flow-density curve (Fig. 4) with a flow value of $q_A = 3397\text{veh/hr/lane}$ and a density value of $\rho_A = 50\text{veh/km/lane}$. A perturbation in the form of a bottleneck/stoplight/accident point is introduced by a modified unit pulse function that indicates an abrupt temporary increase in the traffic density between 8 and 12 km from the normal $\rho_A = 50\text{veh/km/lane}$ to the jam density $\rho_A = 156\text{veh/km/lane}$ (Fig. 6). The simulation is run at 1000 discrete points along a 10-hour time scale and subsequently the system state return time to its initial or other suitable state, which is a resilience indicator, is investigated under various values of the kinematic viscosity (D). The values of D which represent the built-in diffusion/dissipation level within the system are selected between 1 and zero that are consistent with the fluid

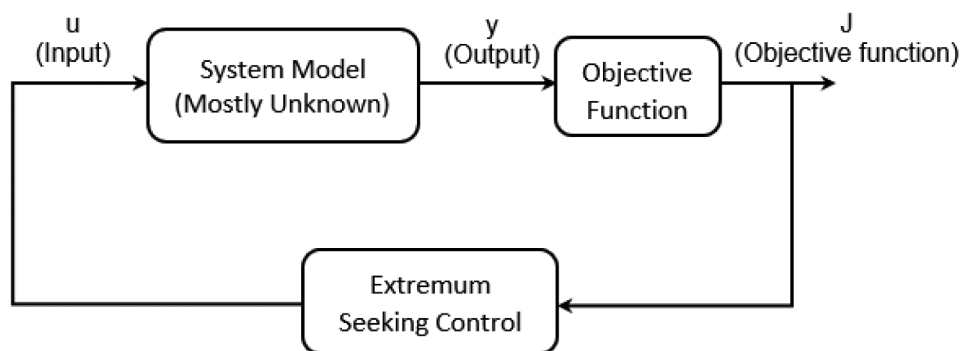


Fig.5 A simplified schematic illustration of an adaptive extremum-seeking controller

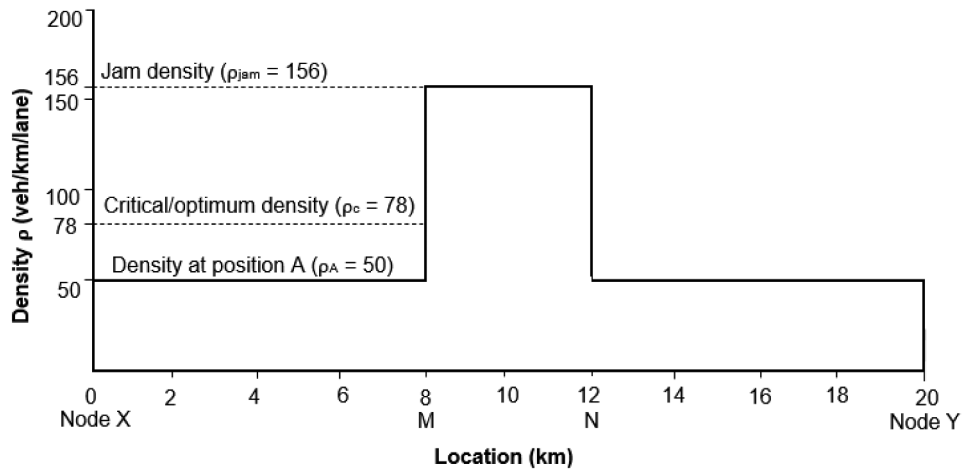


Fig.6 Graphical description of the perturbation density described by a modified unit pulse function around the link mid-point.

dynamics principles. High positive values of D indicate faster dissipation of perturbation/discontinuity in the flow while a zero value indicates no room for the diffusion of a perturbation event.

To simulate the modified viscous Burgers' equation with its distributed system state vector of (flow $q(x, t)$ and density $\rho(x, t)$), a series of Fourier Transform (FT) and Fast Fourier Transform (FFT) operations with some of their inverses are utilized to convert the modified viscous Burgers' equation from its partial differential equation (PDE) form (Eq. 4) into a nonlinear ordinary differential equation (ODE) form (Eq. 13), which is then simulated in the MATLAB environment. The detailed mathematical rigor for FT and FFT operations is omitted for the sake of simplicity.

$$\frac{d}{dt}\rho = -v_f d\rho + 2v_f \frac{\rho}{\rho_{jam}} d\rho + D \cdot d\rho^2 \quad (13)$$

Resilience as the ability of the system state to return to its initial or other suitable state [in the sense of elastic or specified resilience] is quantified by the system state rate of return to equilibrium or the settling time, which is in turn determined by the system dominant eigenvalue or dynamic stability. The system state return ability is rooted in its resistance to perturbation, which is defined by the passive feedback features built into the system. For the subject traffic flow system of the modified viscous Burgers' equation, the ability of the system to resist perturbation is equivalent to the kinematic viscosity (D) in the flow which illustrates how compressible the traffic flow is, and a higher kinematic viscosity (D) value translates into a faster state return rate to equilibrium—resulting in higher resilience and vice versa. For the road physical infrastructure, the kinematic viscosity translates into designing a redundancy margin in the road link geometric components, such as an additional number of lanes

and increased lane width, that could accommodate the predicted additional amount of traffic density caused by the perturbation (bottleneck) without any external intervention (active feedback).

For a kinematic viscosity rate of ($D=1$), (Fig. 7) illustrates a perturbed system state (density) spatial and temporal return to a suitable state (optimum density $\rho_{jam} = 78$) in approximately 3 units of time. The perturbed system's entire state vector trajectory is demonstrated by the system state phase and the system state vector time response (Fig. 8).

For a kinematic viscosity rate of ($D=0.51$), (Fig. 9) illustrates a perturbed system state's (density) spatial and temporal return to a suitable state (optimum density $\rho_{jam} = 78$) in approximately 5 units of time. The perturbed system's entire state vector trajectory is demonstrated by the system state phase and the system state vector time response (Fig. 10). As the values of kinematic viscosity (D) get close to zero, the system starts to lose its ability to handle discontinuity and shockwaves—this abnormality and lack of stability in the flow are visible in the system state variable/output unbounded behavior - going above its theoretical maximum capacity (Fig. 10).

For a kinematic viscosity rate of ($D=0$), the modified viscous Burgers' equation turns into a modified non-viscous Burgers' equation or a modified LWR model, which has no passive feedback mechanism for handling perturbation. For positive non-zero kinematic viscosity ($D>0$), the reason behind the perturbed system state's return to the optimum state (position C on the Greenshields flow-density curve) instead of the initial state (position A- on the Greenshields flow-density curve) is consistent with the traffic flow shockwaves analysis based on the vehicles distance-time diagrams conducted by May [38] where, as a result of a spotlight along a road stretch, various shockwaves such as frontal stationery, backward forming, backward recovery and forward moving shockwaves

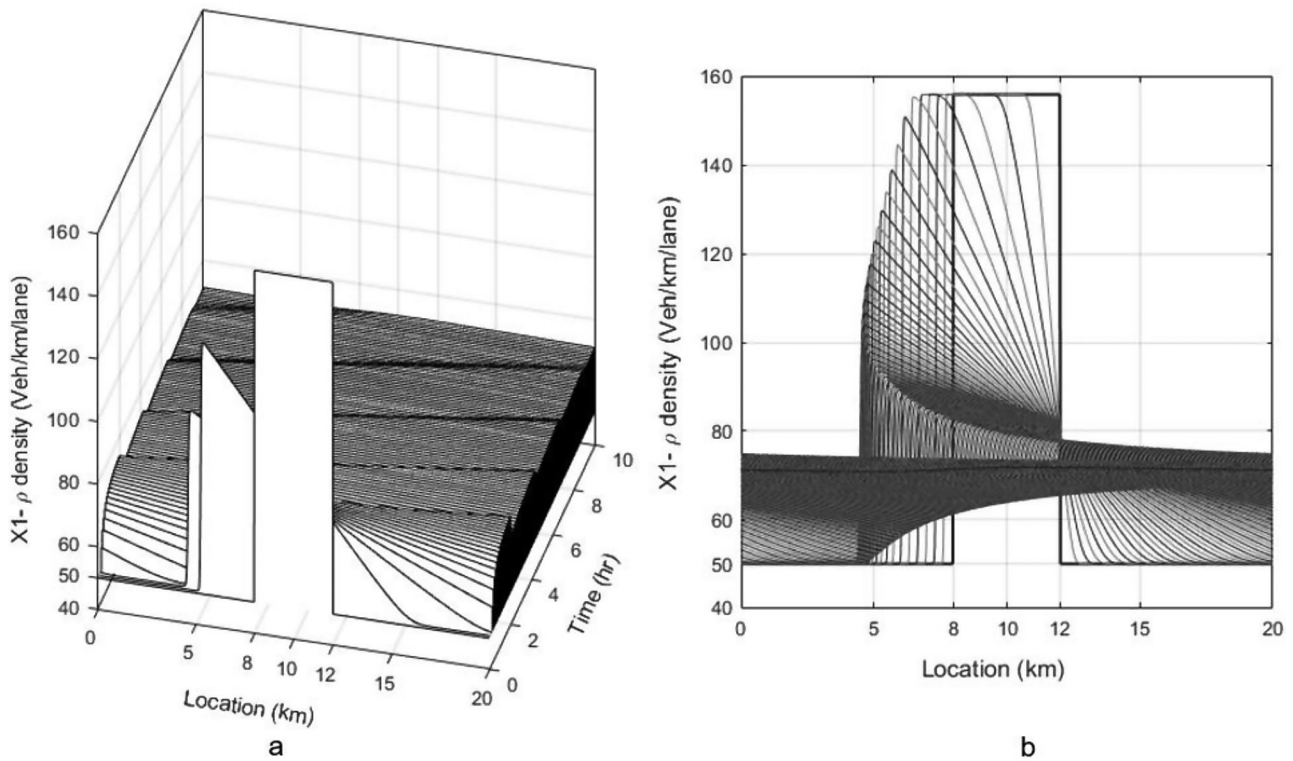


Fig.7 Perturbed system state (density) returns to the optimum suitable state of $\rho_A = 78$ with a 3D (a) and its 2D surface projection (b)

are generated. Similar waves are visible in the simulations conducted for drafting the perturbed system state time evolution (Figs. 7–10).

Resilience as system form return ability

To demonstrate the ability of the system form to return to its initial form or other suitable form, a simple simulation scenario is explored which entails normal vehicular traffic flow moving from node X toward node Y along a two-lane, one-way road section (Link XY of length $L = 12$ km) (Fig. 11). The first Section of the Link XY until the point M (XM) is assumed to be following the LWR- Greenshields constituent equation with a maximum capacity of $q_{max} = 3900$ veh/hr/lane, jam density of $\rho_{jam} = 156$ veh/km/lane, critical or optimum density of $\rho_{cr} = 78$ veh/km/lane, a free flow speed of $v_f = 100$ km and traffic flow in a normal free flow condition (Fig. 4– position A; flow of $q_A = 3397$ veh/hr/lane and density of $\rho_A = 50$ veh/km/lane). At point M, the start of the second Section of the Link XY (MY), a bottleneck (perturbation) reduces the link width to a single lane with a maximum flow of $q_{max} = 1950$ veh/hr/lane, jam density of $\rho_{jam} = 78$ veh/km/lane, critical or optimum density of $\rho_{cr} = 39$ veh/km/lane, and a free flow speed of $v_f = 100$ km; the traffic is assumed to be still following the Greenshields constituent equation (Fig. 11).

When the free-flowing traffic in the first section of the Link XY (flow $q_A = 3397$ veh/hr/lane and density

$\rho_A = 50$ veh/km/lane) is more than the critical flow and density of the second section of the Link XY (flow $q_{cr} = 1950$ veh/hr/lane and density $\rho_{cr} = 39$ veh/km/lane) (Fig. 12), the traffic in the second section of the link will go into a congested state and form and will not return to its initial or other suitable state and form unless an external intervention in the form of active feedback/control is implemented.

In order to keep the traffic flow in the second section of the link XY at its optimum flow conditions ($q_{cr} = 1950$ veh/hr/lane and $\rho_{cr} = 39$ veh/km/lane), an active feedback in the form of adaptive extremum seeking control is implemented (Fig. 13). The controlled upstream traffic density at the left-side of point M (upstream which is calculated as the upstream flow divided by the variable speed limit) is considered as the input and the optimum flow at the downstream or right-side of the point M (downstream) is considered as the output to the objective function. The objective function adopted here is the Greenshields constituent equation (Eq. 14), which has a different form (jam density is reduced at the downstream) to the constituent equation (Eq. 15) followed by the traffic on the first section of the link XY.

$$J = q = 100u - \frac{100}{76}u^2; \rho = u \tag{14}$$

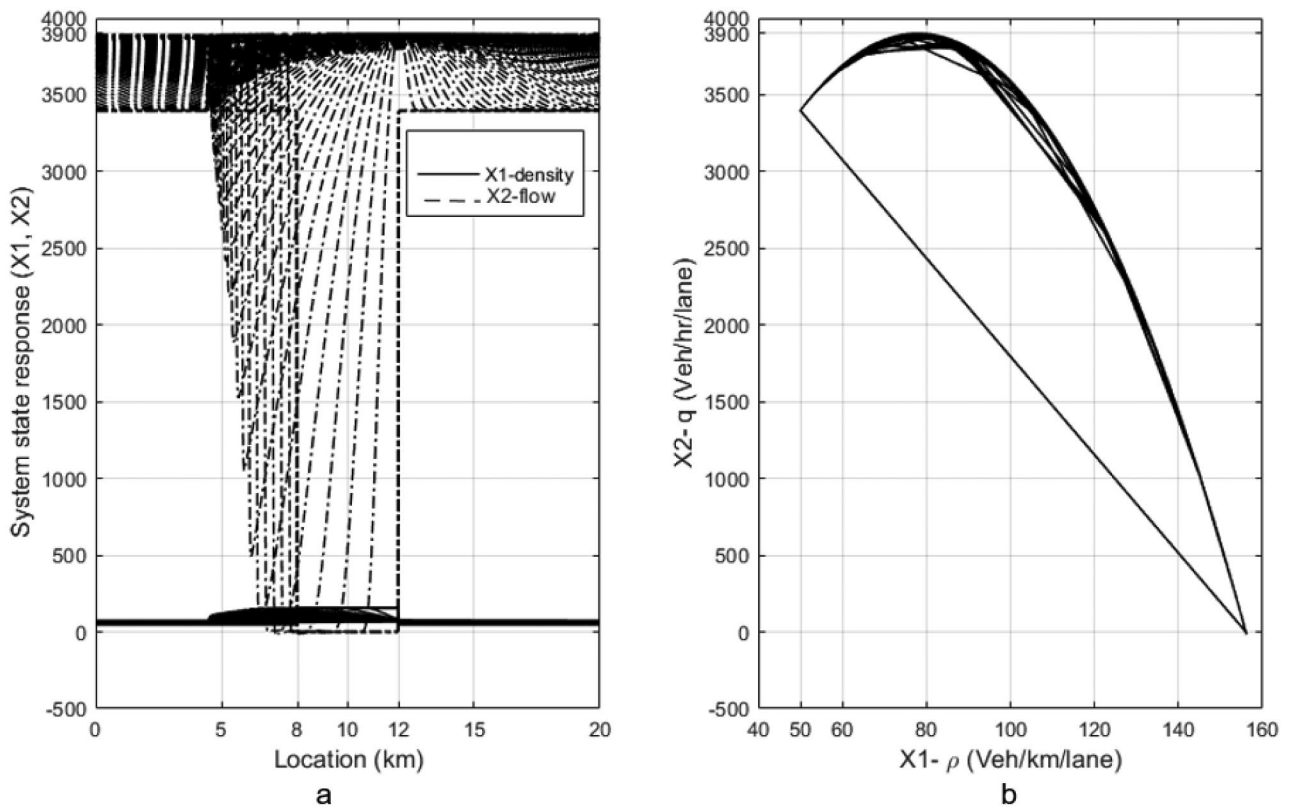


Fig. 8 Perturbed system state vector time response (a) and the system space phase (b) indicating the system state vector return to the optimum state ($\rho_A=78, q_A=3900$) for $D=1$. The density visibility is limited on the scale of Fig. 8a because of its relatively smaller numbers. For full visibility of the same density distribution see Fig. 7b

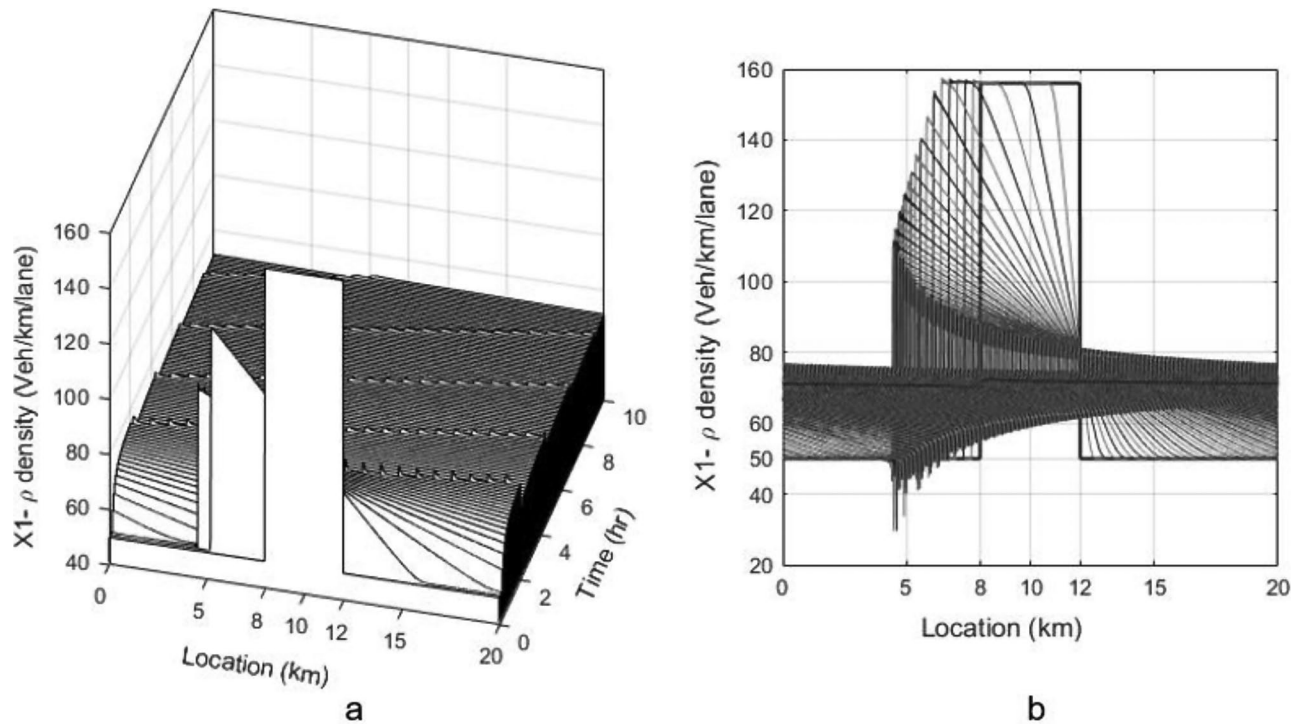


Fig. 9 Perturbed system state (density) returns to the optimum suitable state of $\rho_A=78$ with a 3D (a) and its 2D surface projection (b) graphical illustration for $D=0.51$.

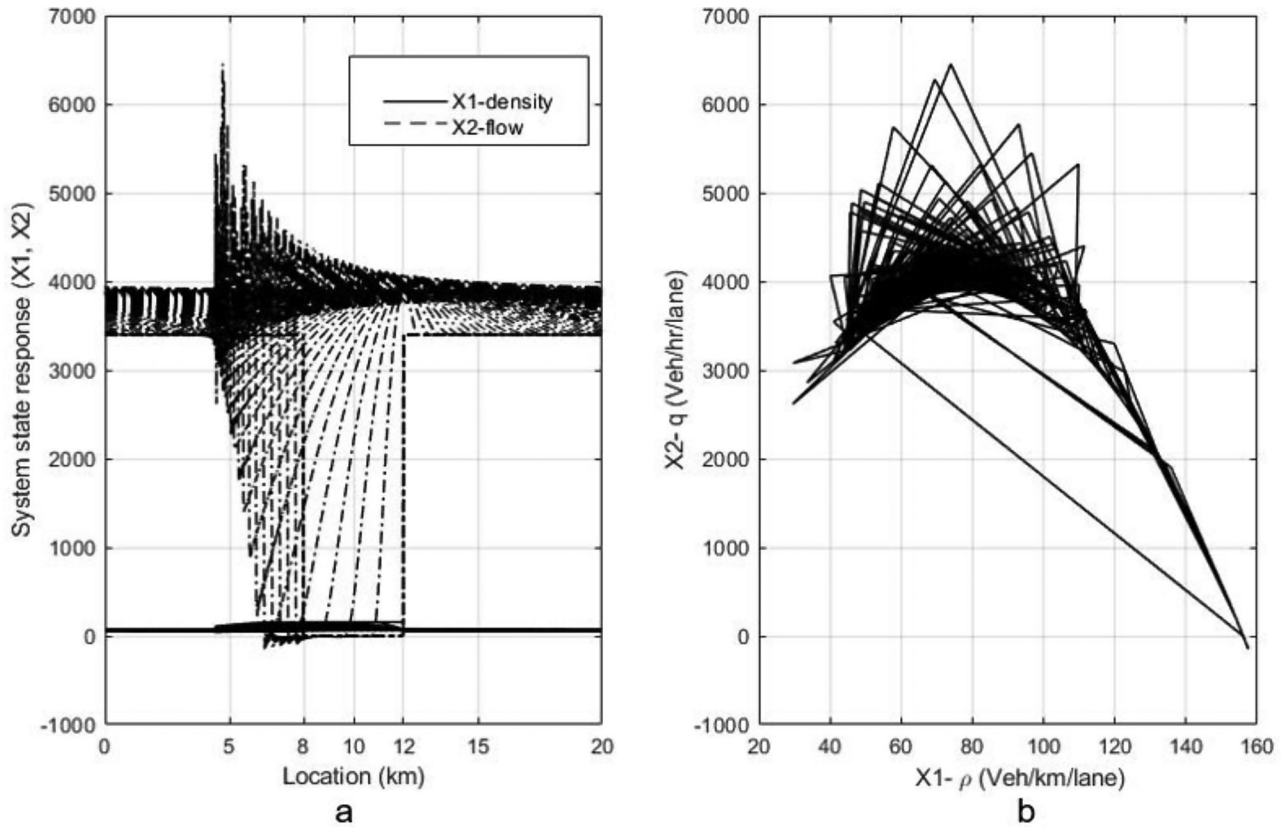


Fig. 10 Perturbed system state vector time response (a) and the system space phase (b) indicating the system state vector return to the optimum state ($\rho_A=78, q_A=3900$) for $D=0.51$. The density visibility is limited on the scale of Fig. 10a because of its relatively smaller numbers. For full visibility of the same density distribution see Fig. 9b

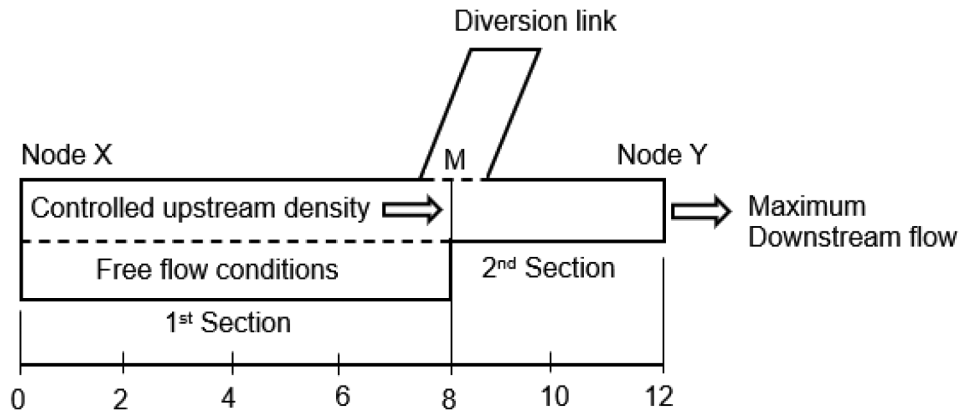


Fig. 11 Schematic illustration of a two-lane highway link's traffic density with a bottleneck and diversion link

$$J = q = 100u - \frac{100}{158}u^2 \quad ; \rho = u \quad (15)$$

A simulation scenario is run for 20 s and subsequently, the upstream density, or control action (input), and the downstream optimum flow, the output (also the system state variable) are plotted against time. The system resilience here is described by the ability of the system to return to its initial or other suitable form

where, in the subject case, the system returns to a new suitable form governed by the second section constituent equation (Eq. 14) and its optimal traffic state ($q_{cr} = 1950\text{veh/hr/lane}$ and $\rho_{cr} = 39\text{veh/km/lane}$) in about 10 s. The additional traffic density (\hat{u} or $\hat{\rho}$), which is indicated on the negative side of the density axis, is in fact the redirected density to a diversion link located at point M (Fig. 14). Adjusting the active control (ESC) parameters will subsequently alter its state return abilities

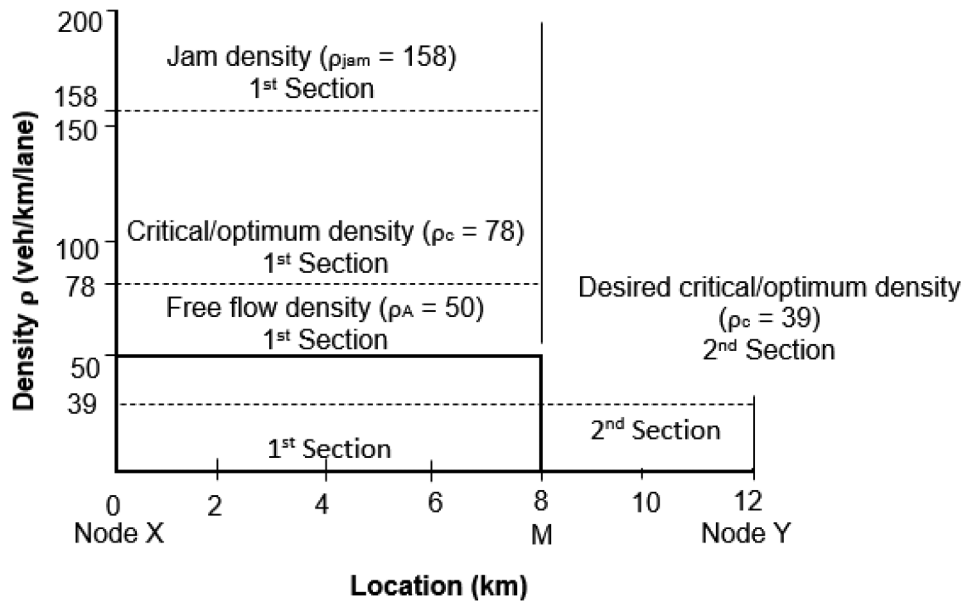


Fig. 12 Graphical description of the perturbation density for the second section (MY) of the link described by a normal traffic flow at the 1st section of the link (XM).

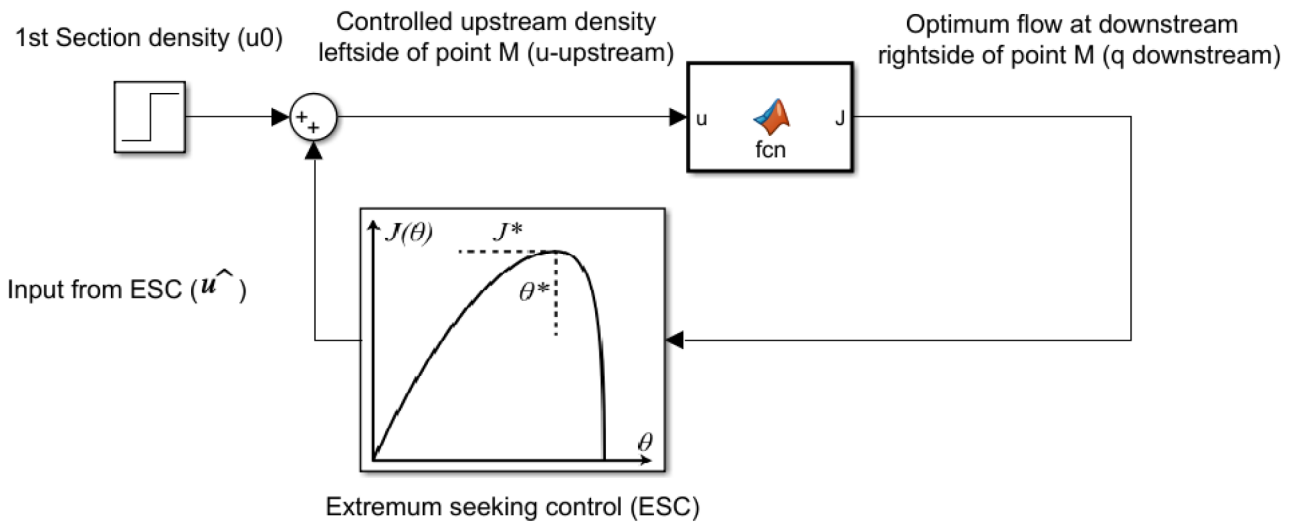


Fig. 13 Schematic illustration of the extremum seeking control at point M of the link XY

in the form of different system settling times. Additionally, the increased robustness and stability of the system feedback/controller mechanism translates into enhanced resilience of the system in the form of resilience. For the physical road infrastructure, this active feedback/control mechanism will translate into road signal regulators such as ramp metering and variable speed limit signs.

Discussion and conclusions

This study demonstrates that the resilience system interpretation framework can be applicable to any system, irrespective of its disciplinary association when defined in terms of control systems rather than by the often

abused and conflicting utilization of the term ‘system(s)’ prevalent in literature. However, this study adopts a single-level system representation for the analysis; the modern control systems approach has the ability to accommodate a more vigorous and detailed multi-level system representation and its subsystem interactions. The two models utilized in this study are simple macroscopic traffic flow systems with homogenous traffic conditions. Whereas for mixed or heterogeneous traffic with variable vehicles, based on the site conditions, a suitable index should be applied to adjust the macroscopic traffic flow system state variables. In absence of the adaptive control measure, traffic in diverging sections- similar

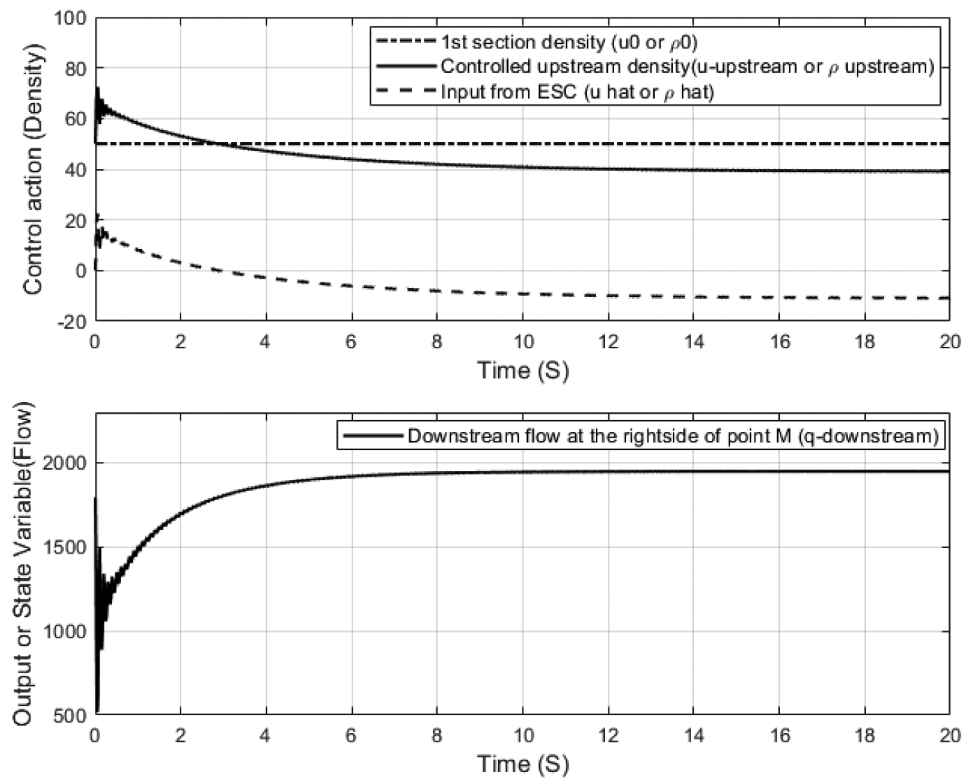


Fig. 14 Control action (u , the upstream density) and the output (q , the downstream optimum flow) time evolution at point M on the link XY

to Fig. 11 might have a resembling or non-resembling behavior to that in section “[Resilience as System Form Return Ability](#)”, given the network layout and the driver’s route choice behavior which is beyond the scope of this study.

As the complexity and uncertainty involved in real-world systems increase, it is not always possible to develop system models based on first principles and the laws of physics. Recent advances in resilience-based designs [39, 40], data science and computer-assisted numerical analysis techniques, particularly big data with easier and cheaper access, have made data-based modeling (grey and black box modeling) convenient and relevant. Thus, the adaptive control systems have become increasingly crucial to the resilience design and analysis process compared to the passive control as-built structures. For more complex traffic flow and transportation systems, additional system variables are introduced to the system state vector, which is selected as per the designed objective. By utilizing system tools such as dynamic mode decomposition (DMD), higher dimension systems can be approximated as lower dimension simple systems. The non-uniqueness of the system state vector is a major strength in the space-models and modern control system techniques.

In this study, resilience as the ability of the system form to return to its initial or other suitable form is

demonstrated by an adaptive extremum seeking control with a static objective function. It has been demonstrated that more realistic dynamic objective functions along with spatial domain variables (through time lagging) can be handled by incorporating the ESC scheme (see also Yu et al. [19]). Other alternative adaptive control schemes include model predictive control (MPC) and model reference adaptive control (MRAC). MPC has the added value of handling constraints (e.g., critical thresholds for the system resilience) and can accommodate a global treatment of the system compared to the local, single domain of attraction, treatment rendered by the ESC scheme. Model reference adaptive control (MRAC) is a more efficient tool for systems with only a single parameter uncertainty, which is more of a robust control scheme compared to the adaptive control. Defining the system and its constituent elements for complex dynamic systems is a critical and challenging task of this methodology which requires a deep understanding of the system as well as the underlying environment in which the system operates. Application of the resilience system interpretation framework to further complex dynamic systems with higher dimensions and multiple perturbations are the some of the potential directions the authors recommend for future research projects.

Acknowledgements

Not applicable.

Author contributions

Conceptualization, K.M. and D.G.C.; methodology and analysis tools, K.M.; background, content analysis and results, K.M.; writing—original draft preparation, K.M.; writing—review and editing, K.M and X.S.; visualization, K.M.; supervision, D.G.C. and X.S. All authors have read and agreed to the published version of the manuscript.

Funding

This study did not receive any specific grant from funding agencies in the public, commercial, or not-for-profit sectors.

Data availability

The datasets used and/or analysed during the current study are available from the corresponding author on reasonable request.

Declarations**Competing interests**

The authors declare no competing interests.

Received: 1 July 2023 / Revised: 5 March 2024 / Accepted: 12 March 2024

References

- Mayar K, Carmichael DG, Shen X (2022) Resilience and Systems—A. Rev Sustain 14:8327. <https://doi.org/10.3390/su14148327>
- Zhang X, Miller-Hooks E, Denny K (2015) Assessing the role of network topology in transportation network resilience. *J Transp Geogr* 46:35–45
- Kurth M, Kozłowski W, Ganin A, Mersky A, Leung B, Dykes J et al (2020) Lack of resilience in transportation networks: economic implications. *Transp Res Part Transp Environ* 86:102419. <https://doi.org/10.1016/j.trd.2020.102419>
- Akbarzadeh M, Memarmontazerin S, Derriche S, Salehi Reihani SF (2019) The role of travel demand and network centrality on the connectivity and resilience of an urban street system. *Transportation* 46:1127–1141. <https://doi.org/10.1007/s11116-017-9814-y>
- Ganin AA, Kitsak M, Marchese D, Keisler JM, Seager T, Linkov I (2017) Resilience and efficiency in transportation networks. *Sci Adv* 3:e1701079. <https://doi.org/10.1126/sciadv.1701079>
- Ni X, Osaragi T, Huang H, Li R, Chen A (2021) Resilience-oriented performance assessment method for road traffic system: a case study in Beijing, China. *KSCE J Civ Eng* 25:3977–3994
- Li Z, Li C, Zhang Y, Hu X (2017) Intelligent traffic light control system based on real time traffic flows. 2017 14th IEEE Annu. Consum. Commun. Netw. Conf. CCNC, IEEE; p. 624–5
- Sommer M (2019) Resilient traffic management: from reactive to proactive systems. University of Augsburg
- Mallah RA, Halabi T, Farooq B Resilience-by-design in adaptive Multi-agent Traffic Control systems. *ArXiv201202675 Cs* 2021.
- Shang W-L, Chen Y, Li X, Ochieng WY Resilience analysis of Urban Road Networks based on adaptive Signal controls: Day-to-Day Traffic dynamics with deep reinforcement learning. *Complexity* 2020;2020:e8841317. <https://doi.org/10.1155/2020/8841317>
- Galkin A, Syssoev A, Khabibullina E (2021) Automation of Traffic Flow Control in Intelligent Transportation Systems. *Reliab. Stat. Transp. Commun.*, Springer, Cham; p. 590–600. https://doi.org/10.1007/978-3-030-68476-1_55
- Byrne RH, Abdallah CT (1995) Design of a model reference adaptive controller for vehicle road following. *Math Comput Model* 22:343–354. [https://doi.org/10.1016/0895-7177\(95\)00143-P](https://doi.org/10.1016/0895-7177(95)00143-P)
- Liu HX, Ban JX, Ma W, Mirchandani PB (2007) Model reference adaptive control framework for real-time traffic management under emergency evacuation. *J Urban Plan Dev* 133:43–50
- Tettamanti T, Varga I, Kulcsár B, Bokor J (2008) Model predictive control in urban traffic network management. 2008 16th Mediterr. Conf. Control Autom., IEEE; pp 1538–1543
- Tettamanti T, Varga I (2009) Traffic control designing using model predictive control in a high congestion traffic area. *Period Polytech Transp Eng* 37:3–8
- Tettamanti T, Varga I, Péni T MPC in urban traffic management. *Model Predict Control* 2010:251–268
- Chavoshi K, Kouvelas A (2020) Nonlinear Model Predictive Control for Coordinated Traffic Flow Management in Highway systems. 2020 Eur Control Conf ECC 428–433. <https://doi.org/10.23919/ECC51009.2020.9143962>
- Pan hongguang, Gao Yxinyu, Li lei, Hua Y W. Model Predictive Control-based multivariable Controller for Traffic flows in Automated Freeway systems. *IEEE Intell Transp Syst Mag* 2022:2–14. <https://doi.org/10.1109/ITS.2022.3182648>
- Yu H, Koga S, Oliveira TR, Krstic M Extremum Seeking for Traffic Congestion Control with a downstream bottleneck. *ArXiv190404315 Math* 2019.
- Tajdari F, Roncoli C, Papageorgiou M (2022) Feedback-based Ramp Metering and Lane-changing Control with Connected and Automated vehicles. *IEEE Trans Intell Transp Syst* 23:939–951. <https://doi.org/10.1109/TITS.2020.3018873>
- Bogenberger K, Keller H, Ritchie SG Adaptive fuzzy systems for traffic responsive and coordinated ramp metering 2001
- Liu H-H, Hsu P-L (2006) Design and simulation of adaptive fuzzy control on the traffic network. 2006 SICE-ICASE int. Jt Conf, IEEE; p. 4961–4966
- Daneshfar F, RavanJamJah J, Mansoori F, Bevrani H, Azami BZ (2009) Adaptive fuzzy urban traffic flow control using a cooperative multi-agent system based on two stage fuzzy clustering. *VTC Spring 2009-IEEE 69th veh. Technol Conf, IEEE*; p. 1–5
- Lin H, Han Y, Cai W, Jin B (2022) Traffic signal optimization based on fuzzy control and differential evolution algorithm. *IEEE Trans Intell Transp Syst*
- Mayar K, Carmichael DG, Shen X (2022) Stability and Resilience—A systematic Approach. *Buildings* 12:1242
- Mayar K, Carmichael DG, Shen X (2023) Resilience and Systems—A Building structure case Example. *Buildings* 13:1520
- Carmichael DG (2013) The conceptual power of control systems theory in engineering practice. *Civ Eng Environ Syst* 30:231–242. <https://doi.org/10.1080/010286608.2013.865021>
- Cascetta E (2009) Transportation systems analysis: models and applications, 2nd edn. Springer, New York
- Carmichael DG (1981) Structural modelling and optimization: a general methodology for engineering and control. Ellis Horwood, Chichester, West Sussex, UK
- Blaauwendraad J, Hoefakker JH (2014) Donnell bending theory for shallow shells. *Struct. Shell Anal*, 1st edn. Springer, United States, pp 73–82
- Elefteriadou L (2014) An introduction to traffic flow theory, 2nd edn. Springer, New York, NY, USA
- Ferrara A, Saccone S, Siri S (2018) Microscopic and mesoscopic traffic models. In: Ferrara A, Saccone S, Siri S (eds) *Free. Traffic Model. Control*, 1st edn. Springer International Publishing, Cham, Switzerland, pp 113–143. https://doi.org/10.1007/978-3-319-75961-6_5
- Peursum S (2015) A study on the behaviour of microscopic car-following models in urban settings. Thesis. Curtin University
- Kachroo P (2018) Pedestrian dynamics: Mathematical Theory and Evacuation Control, 2nd edn. CRC, Boca Raton, Florida. <https://doi.org/10.1201/9781315218359>
- Chowdhury D, Santen L, Schadschneider A (2000) Statistical physics of vehicular traffic and some related systems. *Phys Rep* 329:199–329
- Rosini MD (2013) Macroscopic models for vehicular flows and crowd dynamics: theory and applications, 1st edn. Springer, Cham, Switzerland
- Krstic M, Wang H-H (2000) Stability of extremum seeking feedback for general nonlinear dynamic systems. *Automatica* 36:595–601
- May AD (1990) Traffic flow fundamentals, 1st edn. Prentice-Hall, Inc., Englewood Cliffs
- Forcellini D (2020) A resilience-based methodology to assess soil structure interaction on a benchmark bridge. *Infrastructures* 5:90
- Forcellini D (2022) SRRI Methodology to quantify the seismic resilience of Road infrastructures. *Appl Sci* 12:8945

Publisher's Note

Springer Nature remains neutral with regard to jurisdictional claims in published maps and institutional affiliations.